RESEARCH ARTICLE **ISSN 2738-9898 (Print) ISSN 2738-9901 (Online)**

Engine Performance and Emission Analysis of TiO_2 Nanoparticle-Enhanced Waste Cooking Oil Biodiesel

Milan Neupane[1,†], Shahil Sharma[1,†,*], Prajwal Dahal[1,†], Lochan Kendra Devkota[2], and Rabindra Prasad Dhakal[1,*]

[1] Nepal Academy of Science and Technology (NAST), Khulmaltar, Nepal
[2] Department of Automobile and Mechanical Engineering, Thapathali Campus, Institute of Engineering, Tribhuvan University, Kathmandu, Nepal
* Author to whom correspondence should be addressed; E-Mail: *shahil.sharma@nast.org.np, dhakalrabindra3@gmail.com*
† These authors have contributed equally to the work of this research.

Received : 30 December 2025; Received in revised form : 15 January, 2026; Accepted : 15 January, 2026; Published : 29 January, 2026

Abstract

This study has investigated the effect of Titanium dioxide nanoparticles (TiO_2) on the performance and emission characteristics of a Waste Cooking Oil (WCO) biodiesel-diesel blend. Biodiesel was prepared from WCO using an alkali-catalyzed transesterification process, while TiO_2 nanoparticles were prepared by the sol-gel method and characterized using XRD, UV-Vis spectroscopy, SEM, and EDS. Tests were conducted on a single-cylinder CI engine, operated at 1500 rpm, using neat diesel (D100), B20, and B20 with 50 ppm TiO_2 (B20T50) nanoparticles. The results indicate that the base B20 blend gave marginally lower brake power and brake thermal efficiency compared to diesel, which is mainly due to its lower calorific value. The addition of TiO_2 nanoparticles helped in improving the combustion of fuel, thus giving higher brake power and thermal efficiency and resulting in reduced BSFC under all load conditions. Regarding emissions, biodiesel blends resulted in lesser CO and HC emissions, and further reductions were registered for B20T50. While CO_2 emissions were increased, NO_x emissions decreased compared with the base B20 blend due to improved and controlled combustion characteristics.

Keywords

Waste Oil, Biodiesel Blend, Nanoparticles, Performance Enhancement, Emission Reduction

1. Introduction

Efforts to improve the performance of compression ignition engines increasingly focus on enhancing air-fuel interaction and combustion quality. Among the explored alternative fuels, diesel-biodiesel blends have emerged as a pragmatic option because they preserve the operability of existing diesel engines and at the same time offer clean combustion due to their inherent oxygen content [1]. This oxygenated chemistry generally supports more complete oxidation, which in turn reduces carbon monoxide (CO), particulate matter (PM), and unburned hydrocarbon (HC) emissions under steady load conditions [2]. Still, biodiesel blends can suffer from drawbacks related to lower volatility and higher density, often leading

to slightly higher Brake Specific Fuel Consumption (BSFC) and reduced Brake Power (BP), and Brake Thermal Efficiency (BTE) at increasing engine loads [3].

The last decade has seen rapid growth in the development of biodiesel blends dispersed with trace amounts of functional nanoparticles to address some of these limitations [4]. Metal-oxide nanoparticles have shown high potential in this respect because they change fuel chemistry directly and influence the combustion at microscale as well. Their high specific surface area, thermal conductivity, and catalytic behaviour contribute to enhanced air-fuel mixing, faster heat transfer, and improved oxidation of partially burned species [5]. Various studies have reported that nanoparticles can serve as supplementary oxygen carriers and can accelerate the breakdown of long-chain hydrocarbons, often leading to lower CO and HC emissions and rising BTE in some extent [6], [7], [8].

Among the available metal-oxide nanoparticles, Titanium dioxide (TiO_2) stands out due to its thermal stability, chemical inertness, and widespread use in catalytic oxidation processes [9]. TiO_2 has been shown to improve oxidation reactions under engine-relevant conditions, making it one of the most promising candidates for biodiesel enhancement [10], [11]. Unlike metal nanoparticles that may agglomerate or oxidize rapidly, TiO_2 maintains dispersion stability and remains active across the temperature fluctuations. Even so, existing studies often examine nanoparticle-biodiesel combinations in isolation, leaving limited clarity on the relative contribution of the nanoparticle itself and making it difficult to interpret performance and emission outcomes in a practical and comparative context [5], [12].

What remains notably underexplored is the direct comparison of a commonly adopted biodiesel blend like B20 with and without TiO_2 addition, evaluated alongside neat diesel under identical test conditions. Such a side-by-side dataset is important because B20 is already widely regarded as an operationally stable and industry-favored blend and determining whether nanoparticle enrichment adds meaningful advantages or not, has practical implications. The present work investigates the performance and emission characteristics of neat diesel (D100), 80% diesel + 20% biodiesel (B20), and B20 + 50 ppm TiO_2 NPs (B20T50) in a single-cylinder CI engine across four different loads. The study examines BP, BTE, BSFC, and exhaust emission parameters including CO, CO_2, HC, and NO_x.

2. Methodology

2.1 Chemicals used

Titanium tetra iso propoxide [$Ti(OCH(CH_3)_2)_4$], and iso-propanol [$(CH_3)_2CHOH$], were purchased from SRL, concentrated Nitric acid [HNO_3] was procured from Qualigens, Phenolpthalein and DI-water were sourced from a local chemical supplier.

2.2 Production of Biodiesel

The production of biodiesel began with the collection of Waste Cooking Oil (WCO) from various restaurants in the Lalitpur, Nepal. The crude oil was first subjected to a filtration process to remove food residues and other solid impurities. The quality of the filtered feedstock was then evaluated by determining its Free Fatty Acid (FFA) content using the ISO 660 method, which confirmed a value of 1.89%, below the 2% threshold required for the

subsequent transesterification process. Then, the pre-treated oil was heated to 60°C for the conversion reaction. A catalyst solution was prepared with a methanol-to-oil molar ratio of 6:1 and sodium hydroxide at 1% by weight of the oil. This solution was mixed with the heated oil and the reaction proceeded under stirring for one hour. The mixture was then allowed to settle for 12 hours that resulted in the separation of a top layer of Fatty Acid Methyl Ester (FAME), also referred to as biodiesel, from the bottom glycerol layer. After draining the glycerol, the biodiesel was purified by washing it 3-4 times with warm water and subsequently dried in an oven overnight to remove residual moisture, yielding the final biodiesel fuel which was thoroughly described through the flowchart presented in Figure 1.

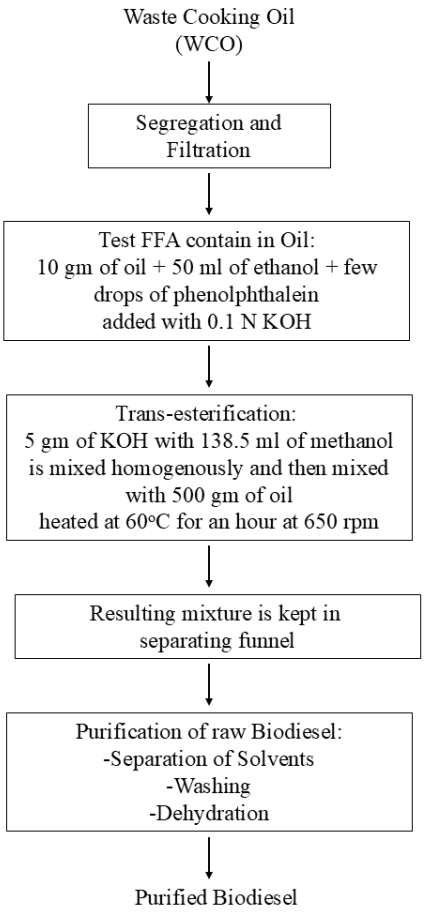

Figure 1: Flow diagram of biodiesel production from waste cooking oil

2.3 Synthesis of TiO_2 NPs

TiO_2 nanoparticles were synthesized using a sol-gel method. In this procedure, 20 ml of Titanium tetra iso propoxide (TTIP) was introduced dropwise into a 22 ml solution containing 10 ml of iso-propanol and 12 ml of deionized water. This mixture was continuously stirred at a temperature of 80°C in a round-bottom flask. After one hour of reaction, a separate mixture of 0.8 ml of concentrated HNO_3 and deionized water was added to the TTIP solution. The combined solution was then maintained at 60°C with constant stirring for 6 hours, resulting in the formation of a highly viscous milky-white gel. This gel was then subjected to a heat treatment at 300°C for 2 hours in an open atmosphere, yielding

white crystalline TiO_2 powder [13]. The synthesis procedure is summarized in the flow diagram presented in Figure 2.

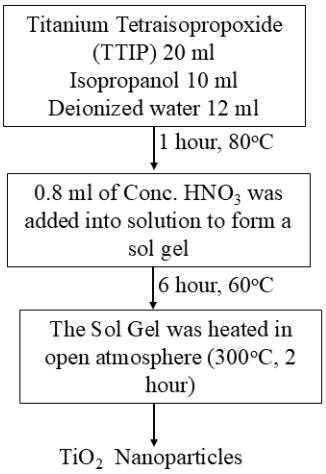

Figure 2: Process flow diagram for the synthesis of TiO_2 nanoparticles

2.4 Physicochemical Properties of Biodiesel

To evaluate key fuel characteristics, B20 biodiesel blend was prepared by mixing 200 ml of the produced biodiesel with 800 ml of conventional diesel. Subsequently, 50 ppm of the synthesized TiO_2 nanoparticles were dispersed into the B20 blend. This mixture was then subjected to one hour of sonication, combined with mechanical stirring, to achieve long-term dispersion stability by preventing agglomeration and ensuring uniform particle distribution in the fuel, creating the nanoparticle-blended fuel (B20T50) [14]. The resulting blend was then analyzed to determine physicochemical properties including calorific value, density, flash point, and kinematic viscosity. These measured parameters, detailed in Table 1, were determined to verify compliance with established fuel standards.

Table 1: Physicochemical properties of Fuels

Property	Standard	Diesel	B100	B20	B20 (with TiO_2 50 ppm)
Calorific Value (kJ/kg)	IP 12/63T	42822.76	38,113.8	41124.14	42644.01
Density@15°C (kg/m^3)	ASTM D 1298/P	828.5	879	843.9	859.09
Flash Point (°C)	ASTM D93	54	136	104	109
Kinematic Viscosity@40°C (cSt)	ASTM D 445/P 25/IP 440	2.87	5.34	3.23	3.31

2.5 Research Engine Setup

A single-cylinder, four-stroke, water-cooled Kirloskar engine with a variable compression ratio was used for experimental testing. The engine maintained a constant speed of 1500 rpm and delivered a rated power output of 3.5 kW, with its technical specifications listed in Table 2. An eddy current dynamometer connected to the engine provided precise torque and speed

measurements. A strain-gauge load cell with a 0-50 kg range was employed to determine the engine load. Performance evaluations were carried out under varying load conditions of 25%, 50%, 75%, and 100%, corresponding to brake loads of approximately 1 kg, 3 kg, 6 kg, and 9 kg respectively.

Table 2: Technical specifications of the test engine

Engine Parameters	Specification
Type	Four-stroke, single cylinder, water-cooled, naturally aspirated, multifuel VCR test engine
Number of cylinders	1
Cylinder Volume capacity	661cc
Max. Engine Power	3.5 kW
Speed	1500 rpm
Compression Ratio	17.5:1

3. Results and Discussion

3.1 Characterization of TiO_2 Nanoparticles

3.1.1 X-Ray Diffraction

Figure 3 illustrates the crystalline structure of the synthesized TiO_2 NPs examined using XRD, and the obtained pattern exhibited well-defined diffraction peaks of TiO_2. A strong and sharp peak observed near $2\theta \approx 27°$ indicates a high degree of crystallinity, while several additional peaks in the range of 30°–70° correspond to the typical reflections of TiO_2 phases. The overall pattern confirms the formation of nanocrystalline TiO_2 with no additional impurity peaks, suggesting high purity of the sample. The broadening of the diffraction peaks further supports the nanoscale dimensions of the particles, consistent with the expected structural features of TiO_2 nanoparticles.

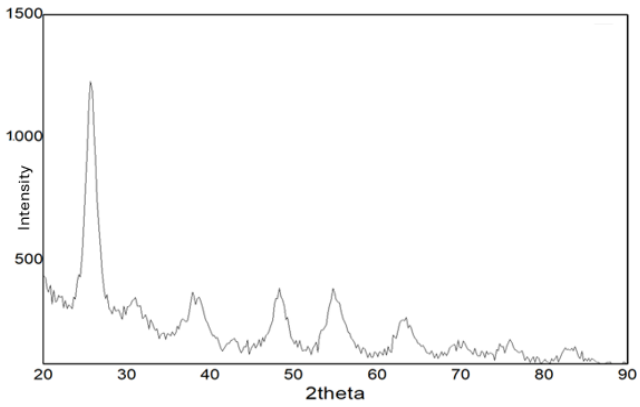

Figure 3: X-ray Diffraction pattern showing characteristic peaks of TiO_2 NPs

3.1.2 UV–visible (UV–Vis) spectroscopy

The optical properties of the synthesized TiO_2 NPs as shown in Figure 4, were investigated using UV–Vis, and the absorbance spectrum shows a strong absorption peak in the UV region around 190–220 nm, attributed to the intrinsic band-to-band transitions of TiO_2. Following the main peak, the absorbance gradually decreases toward the visible region, which is typical for TiO_2 due to its wide band gap and low visible-light absorption. The smooth decay in absorbance beyond 300 nm confirms the absence of additional impurity-

related transitions, indicating good optical purity of the nanoparticles. The spectral profile is consistent with nanoscale TiO_2, where quantum size effects and surface states can slightly influence the absorption edge. This UV–Vis response further supports the successful formation of TiO_2 nanoparticles with characteristic wide-band-gap semiconductor behaviour.

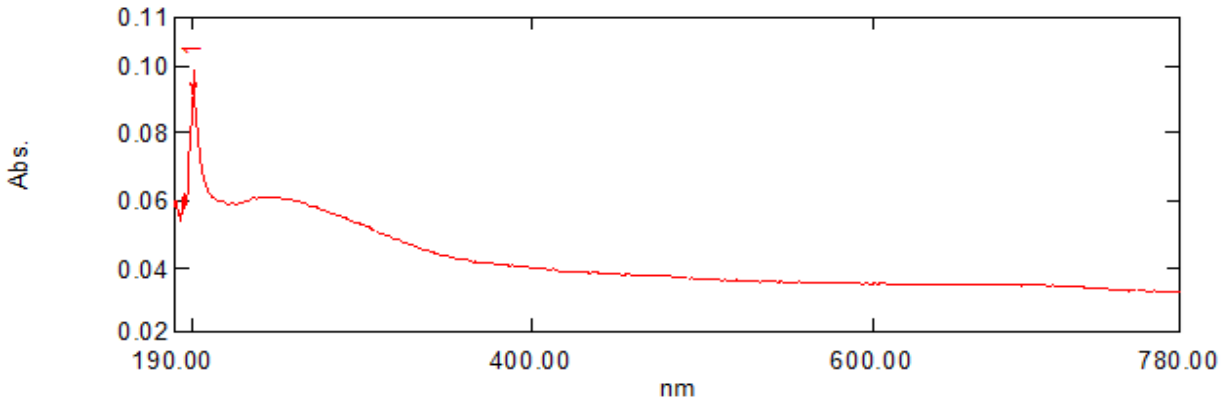

Figure 4: UV-visible absorption spectrum of TiO_2 NPs

3.1.3 Scanning Electron Microscope (SEM)

The SEM micrograph obtained at 20,000X magnification as shown in Figure 5 illustrates TiO_2 nanoparticles with a markedly irregular morphology and a highly textured surface profile. The nanoparticles appear as agglomerated assemblies composed of fine crystallite domains, which create a rough and porous microstructure. Such surface characteristics are beneficial for fuel applications, as the increased surface area enhances catalytic interaction between the nano additive and the fuel molecules. The clustered nanoscale grains also indicate strong surface activity, enabling improved oxidation, better atomization, and more efficient combustion when dispersed in biodiesel. The overall microstructural features suggest that TiO_2 NPs possess the surface reactivity and morphological attributes required for effective performance as a combustion-enhancing biodiesel.

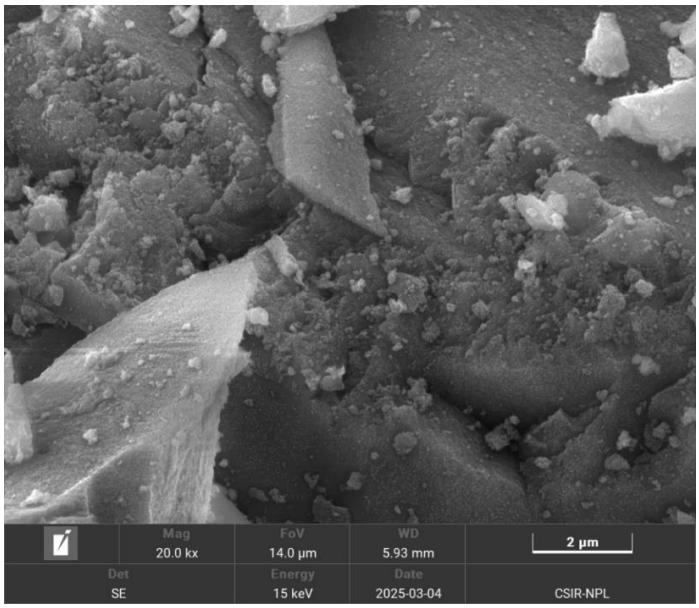

Figure 5: Scanning Electron Microscope image of TiO_2 NPs

3.1.4 Energy - Dispersive X-ray Spectroscopy (EDS)

The EDS spectrum of the synthesized TiO_2 NPs, as shown in Figure 6, exhibits two prominent peaks associated with Oxygen (O) and Titanium (Ti), confirming the formation of TiO_2 without detectable secondary elements. Quantitative elemental analysis shows that the sample contains 53.00 wt.% oxygen (77.14 at%) and 47.00 wt.% titanium (22.86 at%), which closely aligns with the theoretical stoichiometry of TiO_2. The higher atomic percentage of oxygen is consistent with the oxide framework and reflects complete oxidation of the titanium precursor.

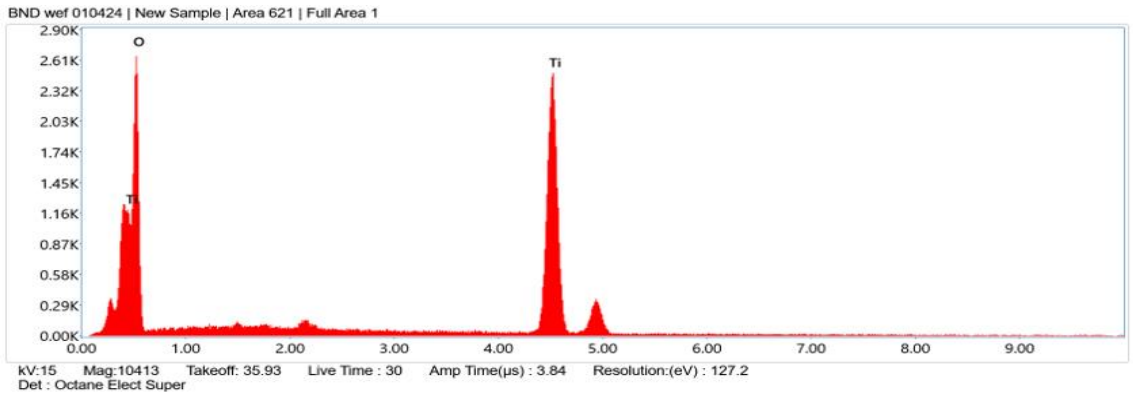

Figure 6: EDS Spectrum of TiO_2 NPs

The absence of unnecessary elemental peaks indicates a high degree of purity in the synthesized nanoparticles, suggesting that the synthesis route effectively minimized contamination or residual precursor species. Such chemical purity is important when TiO_2 is used as a nano additive in biodiesel, as impurities can interfere with catalytic activity or adversely affect combustion characteristics. The measured composition supports the suitability of the prepared TiO_2 for enhancing oxidation reactions, promoting efficient combustion, and potentially improving emission profiles when incorporated into biodiesel blends.

3.2. Performance Characteristics

3.2.1 Brake Power (BP)

The variation of BP with load for D100, B20, and B20T50 is shown in Figure 7. The BP increased with increasing load for all fuels, reflecting the expected rise in fuel consumption and combustion intensity. Across all load conditions, B20 exhibited slightly lower brake power than diesel, primarily due to its lower calorific value. At full load, diesel and B20 delivered 2.61 kW and 2.59 kW, respectively. The B20T50 outperformed both diesel and B20, reaching 2.66 kW.

The improvement in BP with TiO_2 addition can be attributed to the catalytic role of nanoparticles. TiO_2 NP provides additional active oxygen sites, accelerating oxidation reactions, and ensuring more complete combustion of fuel droplets. This behavior has been reported in earlier studies where metal-oxide nanoparticles enhanced in-cylinder combustion by shortening ignition delay and improving flame propagation [10]. Thus, the B20T50 mitigates the performance deficit associated with biodiesel blending.

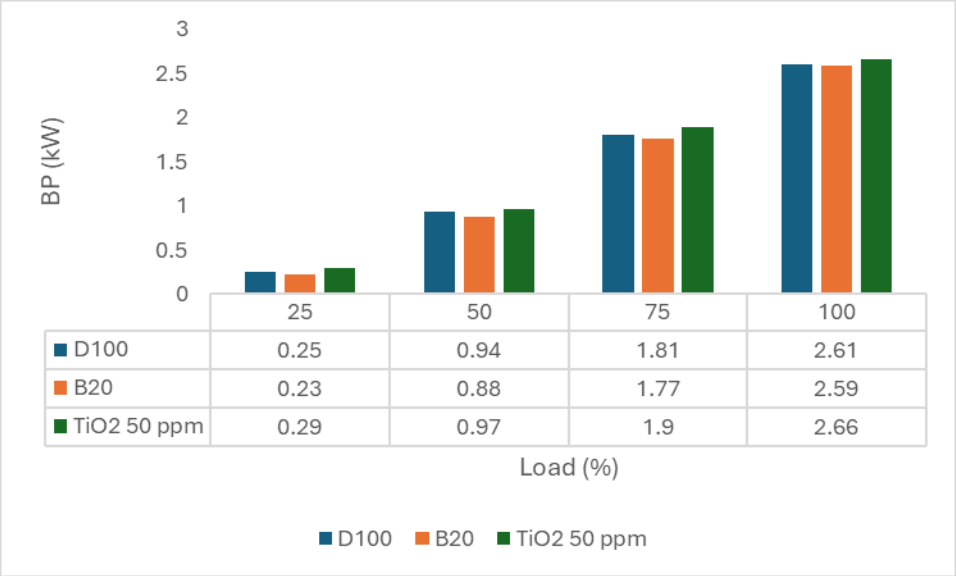

Figure 7: Variation of brake power with engine load for diesel, B20, and B20T50

3.2.2 Brake thermal efficiency (BTE)

BTE trends show a consistent increase with load across all fuels as shown in Figure 8, as higher loads reduce the relative impact of fixed heat and frictional losses [15]. B20 blends recorded a lower BTE compared to diesel, reaching 21.26% and 22.43% respectively at full load. The slight reduction is explained by the lower heating value and higher viscosity of biodiesel, which can reduce atomization and delay combustion phasing [16].

However, the addition of TiO_2 nanoparticles reversed this trend, producing the highest BTE among all fuels tested. At full load, B20T50 blend achieved 23.74%, representing around 6% improvement over D100. At partial loads, similar improvements were observed; for example, at 50% load, B20T50 reached 12.96% compared to 12.47% for diesel and 10.78% for B20. These enhancements are likely due to the oxygen buffering capacity and high surface-to-volume ratio of TiO_2, which promotes more complete combustion of heavier biodiesel molecules [11], [17].

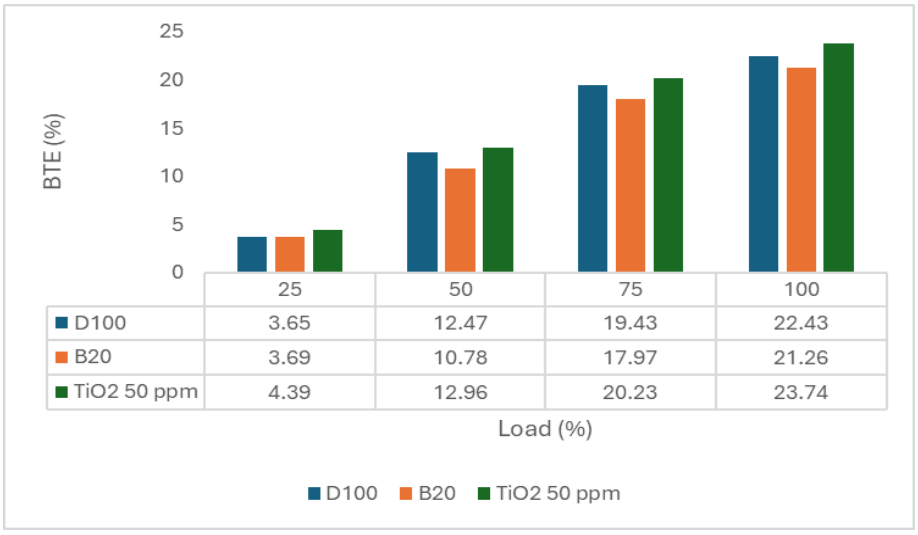

Figure 8: Variation of brake thermal efficiency with engine load for diesel, B20, and B20T50

3.2.3 Brake Specific Fuel Consumption (BSFC)

As illustrated in Figure 9, BSFC decreased with increasing loads for all fuel samples, consistent with improved fuel utilization at higher power outputs. D100 demonstrated lower BSFC than base B20 blends at all loads, which is in line with its higher calorific value. At full load, BSFC values for diesel and B20 were 0.38 and 0.40 kg/kWh, respectively.

B20T50 consistently exhibited the lowest BSFC across the tested load range. At 25% load, BSFC dropped to 1.95 kg/kWh with B20T50 compared to 2.35 kg/kWh for D100. At full load, it recorded 0.33 kg/kWh, representing around 13% and 18% reductions compared to D100 and B20, respectively. These reductions indicate that nanoparticle addition improves the fuel conversion process, allowing less fuel to be consumed per unit of work. Similar results have been noted in previous nanoparticle-assisted biodiesel combustion studies, where TiO_2 and CeO_2 improved atomization and reduced unburned hydrocarbon losses [18], [19].

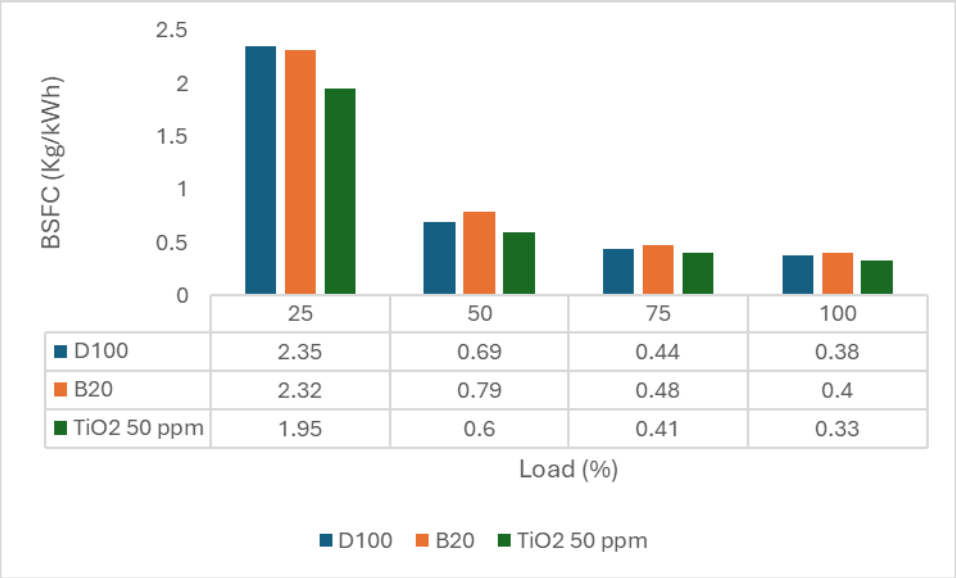

Figure 9: Variation of Brake Specific Fuel Consumption with engine load for diesel, B20, and B20T50

3.2.4 Exhaust Gas Temperature (EGT)

Exhaust gas temperature profiles as shown in Figure 10 rose steadily with increasing load for all fuels, reflecting greater fuel injection, combustion rates, and heat release. At full load, D100 exhibited the highest base-fuel EGT of 331.7 °C, while B20 recorded a substantially lower 285.3 °C. The lower EGT of B20 may be attributed to its oxygenated nature and lower calorific value, which results in slower and cooler combustion.

The B20T50, however, produced the highest EGT across all load points, reaching 348.1 °C at full load. The elevated EGT suggests intensified combustion caused by the catalytic activity of TiO_2 NPs, which accelerate oxidation reactions and promote higher in-cylinder temperatures. While this indicates improved combustion quality, it also highlights a potential trade-off i.e. higher EGTs could increase NO_x formation. Previous reports also emphasize that nanoparticle additives, while improving efficiency, may elevate thermal stress and NO_x emissions due to higher combustion temperatures [20], [21].

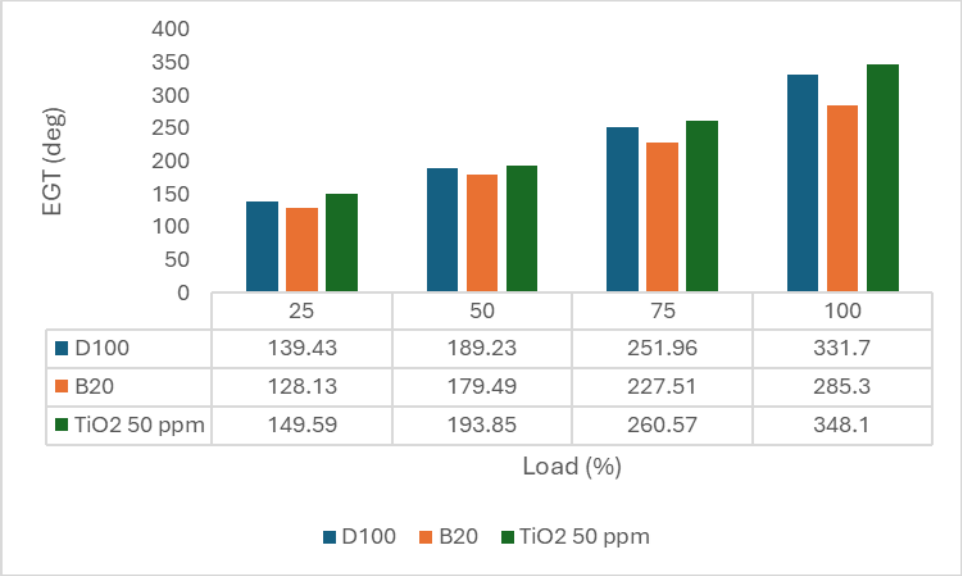

Figure 10: Variation of Exhaust Gas Temperature with engine load for diesel, B20, and B20T50

3.3. Emission Characteristics

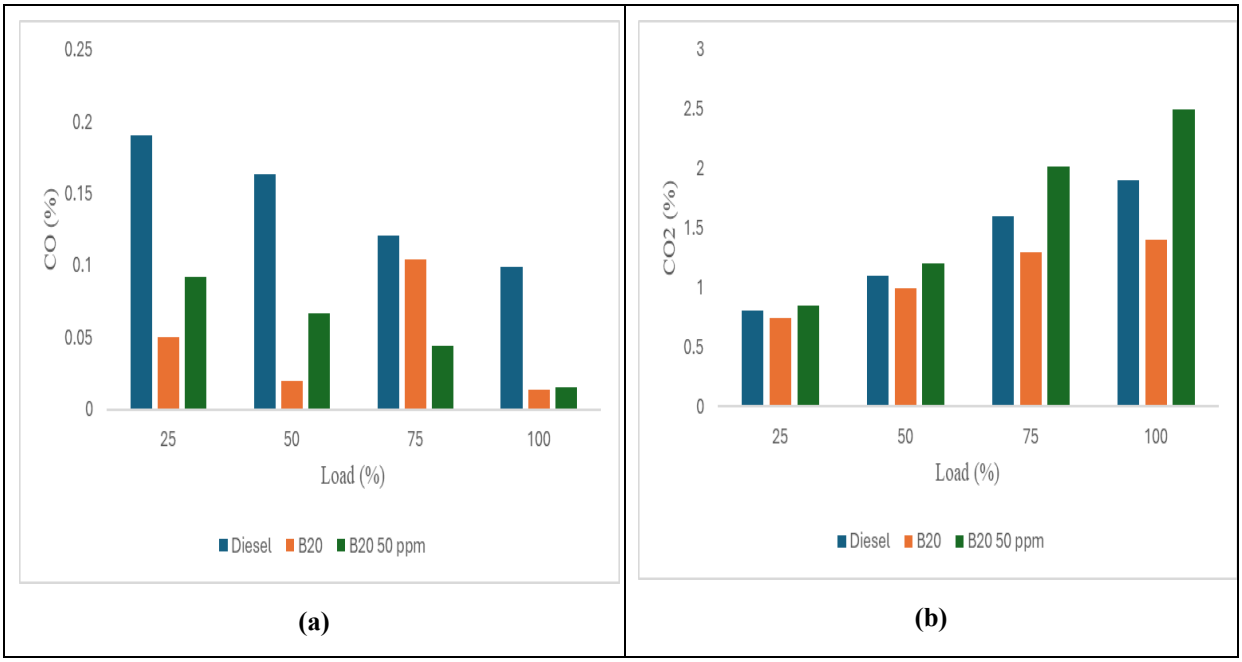

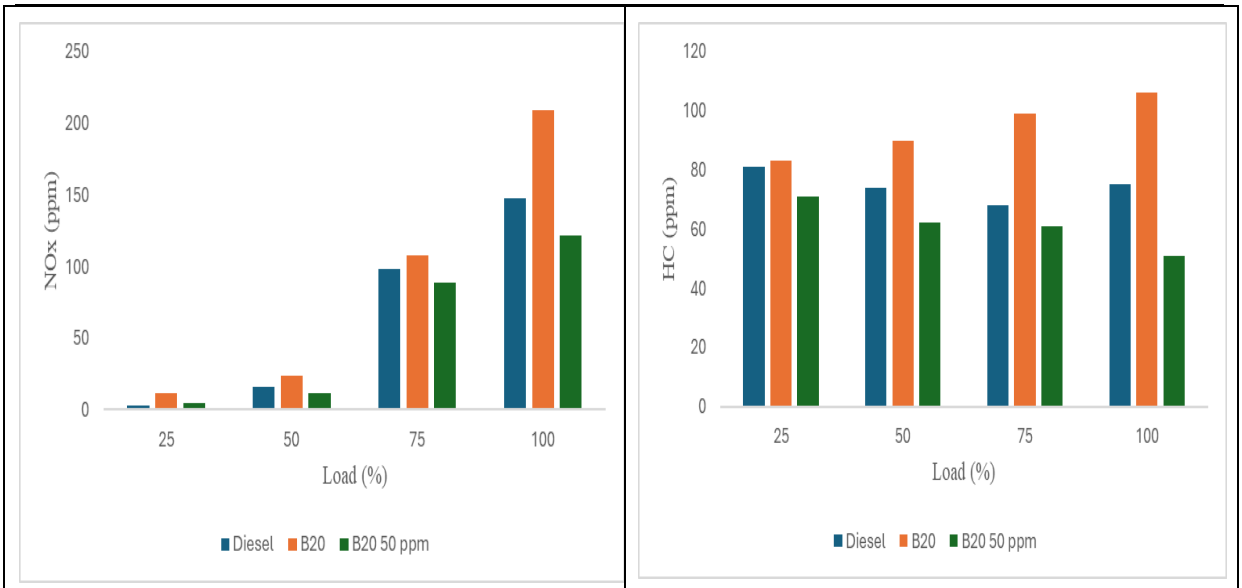

Figure 11: Effect of TiO_2 nanoparticles on (a) CO, (b) CO_2, (c)NO_x, and (d) HC emissions

3.3.1 Carbon Monoxide (CO)

The variation of CO emission with engine load for all test fuels is presented in Figure 11a. Across the entire load range, CO concentration decreases consistently with increasing load for all fuels, which is consistent with the typical combustion behavior of compression-ignition engines. At low load (25%), incomplete combustion dominates due to lower in-cylinder temperatures and reduced air–fuel mixing efficiency, resulting in higher CO levels. As the load increases, higher in-cylinder temperatures promote more complete oxidation of CO to CO_2, leading to lower CO concentrations.

Among the tested fuels, B20 exhibited the lowest CO emissions, followed closely by the B20T50. At full load, CO decreased from 0.10% for D100 to 0.01% for both biodiesel blends, marking a reduction of nearly 90%. The presence of oxygen molecules in biodiesel aid in the oxidation of CO to CO_2, thereby lowering CO emissions. The slight difference between B20 and B20T50 at lower loads (0.05% and 0.09% respectively at 25%) may be attributed to localized temperature effects and initial poor atomization; however, as load increases, the B20T50 consistently maintains lower CO due to the catalytic oxidation effects of TiO_2 NPs. Similar behavior has been reported by [5], [11], [22], [23], who observed that metal-oxide nanoparticles enhance the oxidation kinetics of CO by providing additional oxygen radicals and improving combustion homogeneity.

3.3.2 Carbon Dioxide (CO_2)

CO_2 emission, an indicator of combustion completeness, exhibited an increasing trend with rising load for all fuels, as depicted in Figure 11b. The B20T50 blend recorded the highest CO_2 emissions at all loads, reaching 2.50% at full load, compared to 1.91% for D100 and 1.46% for B20. This suggests more complete combustion due to TiO_2 NPs, supported by the concurrent decrease in CO and HC levels.

The elevated CO_2 concentration in the nanoparticle-doped blend can be attributed to the enhanced oxidation and improved air–fuel mixing induced by TiO_2 NPs catalytic surface activity and oxygen-releasing nature. A similar enhancement in CO_2 was observed by [24], [25] in TiO_2 - added biodiesel (B20T50) combustion, where improved combustion efficiency led to higher CO_2 formation. Therefore, the observed rise in CO_2 corroborates the improvement in brake thermal efficiency noted earlier.

3.3.3 Nitrogen Oxides (NOx)

The NO_x emission trend, presented in Figure 11c, increased with load for all fuels, consistent with the rise in in-cylinder temperature and pressure at higher engine loads. However, the B20T50 showed a notable reduction in NO_x compared to both D100 and B20, particularly at medium and high loads. At full load, NO_x dropped from 148 ppm for D100 and 209 ppm for B20 to 122 ppm for B20T50, representing a reduction of approximately 41% relative to B20.

Although biodiesel blends are generally reported to increase NO_x emissions due to higher combustion temperatures and oxygen content, the observed reduction here can be rationalized by the effects of TiO_2 NPs: their high specific heat capacity can absorb part of the released combustion heat, moderating peak flame temperatures; and improved atomization and shorter combustion duration limit the exposure time of nitrogen and oxygen at high temperatures. Moreover, the modest rise in exhaust gas temperature observed in Figure 10 suggests that the in-cylinder peak temperature likely remained below the critical threshold (~1800 K) required for exponential NO_x formation through the Zeldovich mechanism [26], [27].

3.3.4 Unburned Hydrocarbons (HC)

The HC emissions for all fuel decreased with increasing load, a typical trend in CI engines due to elevated temperatures and longer residence times at higher loads, as shown in Figure 11d. D100 recorded the highest HC values across all loads, while B20T50 consistently exhibited the lowest, decreasing from 71 ppm at 25% load to 51 ppm at full load. This represents roughly a 32% reduction relative to neat diesel at full load (75 ppm).

The reduction in HC emissions in biodiesel blends is due to the oxygenated nature of the fuel, which promotes better oxidation of unburnt hydrocarbons. The additional improvement in the TiO_2 blend arises from the catalytic and micro-explosion effects of NPs, which enhance droplet breakup and increase the local combustion rate. Similar reductions have been observed in prior works by [28], where TiO_2 NPs in biodiesel blends significantly reduced unburnt hydrocarbon emissions due to accelerated oxidation and better charge homogeneity.

4. Conclusions

This research work studied the influence of TiO_2 NPs upon the performance and emissions of waste cooking oil biodiesel and diesel blends in a single-cylinder CI engine. The prepared TiO_2 NPs possess excellent crystallinity and purity along with desired surface characteristics and hence can be applied as an additive for enhancing the characteristics of Biodiesel. The results from engine performance test showed that the BP and BTE for the B20 blend were lower than those for the D100 fuel due to its lower calorific value and higher viscosity. The B20T50 blend gave the highest BP and BTE at all loads with the lowest brake specific fuel consumption. Emission analysis also verified the environmental benefits of B20, with

substantially reduced levels of CO and HC when compared to D100 fuel. Adding the TiO_2 NPs also helped to lower the emissions further.

Conflicts of Interest Statement

The Authors declare that they have no financial interests or personal relationships that could have influenced the research presented in this paper.

Data Availability Statement

The data supporting the findings of this study are presented in the manuscript. Additional data will be provided upon request.

Acknowledgements

The authors would like to acknowledge Bioenergy and Waste Recycling Laboratory at Nepal Academy of Science and Technology (NAST) and Department of Automobile and Mechanical Engineering at Thapathali Campus for providing the necessary laboratory and testing facilities.

References

1. S. P. Adhikari, R. L. Karn, S. Bhushal, L. Palikhel, and S. Bhattarai, "Energy Balance Sheet of Blends of Jatropha Biodiesel at Variable Injection Hole Number in a Single-Cylinder Diesel Engine-An Experimental Approach," *International Journal of Heat and Technology*, vol. 43, no. 2, pp. 751–759, Apr. 2025, doi: 10.18280/IJHT.430234.
2. Y. Zhang, Y. Zhong, S. Lu, Z. Zhang, and D. Tan, "A Comprehensive Review of the Properties, Performance, Combustion, and Emissions of the Diesel Engine Fueled with Different Generations of Biodiesel," Processes 2022, Vol. 10, Page 1178, vol. 10, no. 6, p. 1178, Jun. 2022, doi: 10.3390/PR10061178.
3. K. R. Bhatta, R. L. Karna, A. K. Jha, and S. P. Adhikari, "Performance and Emission Characteristics of Jatropha Biodiesel Blends in a Direct Injection CI Engine," Himalayan Journal of Applied Science and Engineering, vol. 2, no. 2, pp. 24–33, Nov. 2021, doi: 10.3126/HIJASE.V2I2.43393.
4. V. Modi et al., "Nanoparticle-enhanced biodiesel blends: A comprehensive review on improving engine performance and emissions," Mater Sci Energy Technol, vol. 7, pp. 257–273, Jan. 2024, doi: 10.1016/J.MSET.2024.02.001.
5. P. P. Borthakur, "Nanoparticle enhanced biodiesel blends: Recent insights and developments," Hybrid Advances, vol. 10, p. 100442, Sep. 2025, doi: 10.1016/J.HYBADV.2025.100442.
6. V. Kumar and A. K. Choudhary, "Prediction of the Performance and emission characteristics of diesel engine using diphenylamine Antioxidant and ceria nanoparticle additives with biodiesel based on machine learning," Energy, vol. 301, p. 131746, Aug. 2024, doi: 10.1016/J.ENERGY.2024.131746.
7. M. A. Mujtaba et al., "Comparative study of nanoparticles and alcoholic fuel additives-biodiesel-diesel blend for performance and emission improvements," Fuel, vol. 279, p. 118434, Nov. 2020, doi: 10.1016/J.FUEL.2020.118434.
8. S. Gowthaman, A. I. Anu Karthi Swaghatha, K. Thangavel, L. Muthulakshmi, and P. Paramasivam, "Effect of ZnO nanoparticle on combustion and emission characteristics of a diesel engine powered by lemongrass biodiesel: an experimental approach," Discover Applied Sciences 2024 6:7, vol. 6, no. 7, pp.

344-, Jun. 2024, doi: 10.1007/S42452-024-06045-3.

9. S. Bagheri, N. Muhd Julkapli, and S. Bee Abd Hamid, "Titanium dioxide as a catalyst support in heterogeneous catalysis," ScientificWorldJournal, vol. 2014, 2014, doi: 10.1155/2014/727496.
10. H. L. Allasi, A. J. Selvam, M. V. Soosaimariyan, and S. J. Arul, "Enhancing diesel engine efficiency with waste cooking oil biodiesel and nano additives for sustainable fuel applications," Scientific Reports 2025 15:1, vol. 15, no. 1, pp. 31762-, Aug. 2025, doi: 10.1038/s41598-025-17528-7.
11. R. Khujamberdiev and H. M. Cho, "Evaluation of TiO2 Nanoparticle-Enhanced Palm and Soybean Biodiesel Blends for Emission Mitigation and Improved Combustion Efficiency," Nanomaterials 2024, Vol. 14, Page 1570, vol. 14, no. 19, p. 1570, Sep. 2024, doi: 10.3390/NANO14191570.
12. Y. Chen et al., "A comprehensive review of stability enhancement strategies for metal nanoparticle additions to diesel/biodiesel and their methods of reducing pollutant," Process Safety and Environmental Protection, vol. 183, pp. 1258–1282, Mar. 2024, doi: 10.1016/J.PSEP.2024.01.052.
13. A. Sharma, R. K. Karn, and S. K. Pandiyan, "Synthesis of TiO 2 Nanoparticles by Sol-gel Method and Their Characterization," vol. 1, no. 9, pp. 1–5, 2014, Accessed: Dec. 17, 2025. [Online]. Available: http://www.krishisanskriti.org/jbaer.html
14. Y. zhen Lv, C. Li, Q. Sun, M. Huang, C. rong Li, and B. Qi, "Effect of Dispersion Method on Stability and Dielectric Strength of Transformer Oil-Based TiO2 Nanofluids," Nanoscale Res Lett, vol. 11, no. 1, Dec. 2016, doi: 10.1186/S11671-016-1738-5.
15. M. Koirala, A. K. Sah, R. P. Dhakal, R. L. Karn, M. Khanal, and S. P. Adhikari, "Effect of green synthesized zinc oxide nanoadditives and rice bran oil biodiesel blend on performance and combustion characteristics of a variable compression ratio diesel engine: an experimental study," Biofuels, Bioproducts and Biorefining, vol. 17, no. 6, pp. 1595–1610, Nov. 2023, doi: 10.1002/BBB.2527
16. N. G. Mengistu, M. W. Mekonen, Y. G. Ayalew, L. F. Demisie, and T. Nega, "Experimental investigation on diesel engine performance and emission characteristics using waste cooking oil blended with diesel as biodiesel fuel," Discover Energy 2024 4:1, vol. 4, no. 1, pp. 26-, Nov. 2024, doi: 10.1007/S43937-024-00051-7.
17. A. Atmaca and M. A. Kallioğlu, "Titanium dioxide (TiO2) nanoparticle effects on diesel engine efficiency and emission control: A comprehensive study with RSM modelling," Fuel, vol. 404, p. 136228, Jan. 2026, doi: 10.1016/J.FUEL.2025.136228.
18. S. Tamrat, V. R. Ancha, R. Gopal, R. B. Nallamothu, and Y. Seifu, "Emission and performance analysis of diesel engine running with CeO2 nanoparticle additive blended into castor oil biodiesel as a substitute fuel," Scientific Reports 2024 14:1, vol. 14, no. 1, pp. 7634-, Apr. 2024, doi: 10.1038/s41598-024-58420-0.
19. M. S. Gad, H. M. A. Hashish, A. K. Hussein, M. B. Ben Hamida, R. Abdulkader, and M. H. Nasef, "Effect of different configurations of hybrid nano additives

blended with biodiesel on CI engine performance and emissions," Scientific Reports 2024 14:1, vol. 14, no. 1, pp. 19528-, Aug. 2024, doi: 10.1038/s41598-024-69957-5.

20. A. I. EL-Seesy, H. Kosaka, H. Hassan, and S. Sato, "Combustion and emission characteristics of a common rail diesel engine and RCEM fueled by n-heptanol-diesel blends and carbon nanomaterial additives," Energy Convers Manag, vol. 196, pp. 370–394, Sep. 2019, doi: 10.1016/J.ENCONMAN.2019.05.049.
21. H. Khan et al., "Effect of Nano-Graphene Oxide and n-Butanol Fuel Additives Blended with Diesel—Nigella sativa Biodiesel Fuel Emulsion on Diesel Engine Characteristics," Symmetry 2020, Vol. 12, Page 961, vol. 12, no. 6, p. 961, Jun. 2020, doi: 10.3390/SYM12060961.
22. G. Jayabalaji and P. Shanmughasundaram, "Effect of Titanium Dioxide (Tio2) Nano-Fluid on Performance and Emission Features of a Diesel Engine Operated on Aphanizomenon Flos Biodiesel-Diesel Blend," Materials Science Forum, vol. 969, pp. 421–426, 2019, doi: 10.4028/WWW.SCIENTIFIC.NET/MSF.969.421.
23. P. Gunasekar, S. Manigandan, N. Ilangovan, S. Nithya, J. Devipriya, and W. S. R. Saravanan, "Effect of TiO2 and nozzle geometry on diesel emissions fuelled with biodiesel blends," International Journal of Ambient Energy, vol. 40, no. 5, pp. 477–481, Jul. 2019.
24. K. Fangsuwannarak, T. Fangsuwannarak, and Y. Khotbut, "Effect of Nano-TiO2 Additives Blended in Palm Biodiesel on Compression Ignition Engine Performance," Journal of Clean Energy Technologies, vol. 8, no. 3, pp. 20–23, Jul. 2020.
25. R. J. Madhuri, J. V. Naik, and V. Roa, "Effects of Aloe Vera Biodiesel Blends with TiO2 on the Emission and Performance Characteristics of a DI Diesel Engine," Biotechnology Journal International, vol. 27, no. 1, pp. 1–7, Jan. 2023, doi: 10.9734/BJI/2023/V27I1667.
26. I. -I. J. of S. T. and Engineering, "Design of Catalytic Converter for Mitigation of Nox in CI Engine: A Review." Accessed: Dec. 14, 2025. [Online]. Available: https://www.academia.edu/37647516/Design_of_Catalytic_Converter_for_Mitigation_ of_NO_x_in_CI_Engine_A_Review
27. S. Wu, D. Che, Z. Wang, and X. Su, "NOx Emissions and Nitrogen Fate at High Temperatures in Staged Combustion," Energies 2020, Vol. 13, Page 3557, vol. 13, no. 14, p. 3557, Jul. 2020, doi: 10.3390/EN13143557.
28. A. Jain et al., "Assessment of Nahar biodiesel with TiO2 nanoparticles at increased fuel injection pressure of a diesel engine: Exergy, energy, statistical analysis," Case Studies in Thermal Engineering, vol. 71, p. 106125, Jul. 2025, doi: 10.1016/J.CSITE.2025.106125.